Dynamic Stability of a Buoyant Quad-Rotor Aircraft

B.L. Nagabhushan*
Goodyear Aerospace Corporation, Akron, Ohio

Stability characteristics of a buoyant quad-rotor aircraft in hover and forward flight are examined by considering linear, state-variable, and nonlinear flight simulation models of such a vehicle configuration. The effects of carrying a sling load on the aircraft dynamics is predicted by considering a coupled model of the two bodies. Inherent stability characteristics of the vehicle are analyzed and compared with those of a conventional helicopter and an airship in free flight. Typical operational conditions that could lead to aircraft instability are described in the flight envelope of interest.

Nomenclature

A = system matrix
$I_{xx,yy,zz}$ = moment of inertia about reference body axes system whose origin is at the vehicle center of mass
j = $\sqrt{-1}$
K = sling load aerodynamic drag constant (drag = KV_p^2)
l = length of the sling cable, ft
L = rolling moment, ft-lb
M = pitching moment, ft-lb
N = yawing moment, ft-lb
p = roll velocity of the vehicle, rad/s
q = pitch velocity of the vehicle, rad/s
r = yaw velocity of the vehicle, rad/s
$T_{1/2}$ = time to half amplitude, s
u = longitudinal component of the vehicle translational velocity in the x direction of reference body axes, ft/s
u_p = longitudinal component of sling load velocity relative to the aircraft in the x direction of vehicle reference body axes, ft/s
v = lateral component of the vehicle translational velocity in the y direction of reference body axes, ft/s
v_p = lateral component of sling load velocity relative to the aircraft in the y direction of vehicle reference body axes, ft/s
V_p = total velocity of the sling load, ft/s
w = vertical component of the vehicle translational velocity in the z direction of reference body axes, ft/s
x,y,z = coordinates of a point in the reference body axes system, ft
x_p,y_p = coordinates of the sling load in the vehicle reference body axes system, ft
$\bar{x}$ = state vector
$\dot{\bar{x}}$ = derivative of state vector with respect to time
X,Y,Z = components of external forces along the x, y, and z axes, respectively, of the vehicle reference body axes system, lb
z_s = z coordinate of sling load suspension point on the vehicle, ft
Δ = prefix used for small perturbation
θ = pitch attitude of the vehicle, rad
σ = real part of the eigenvalue, rad/s
ϕ = roll attitude of the vehicle, rad
ψ = yaw attitude of the vehicle, rad
ω = circular frequency, rad/s

Received Oct. 26, 1981; presented as Paper 82-0242 at the AIAA 20th Aerospace Sciences Meeting, Orlando, Fla., Jan. 11-13, 1982; revision received June 1, 1982.

*Engineer Specialist, Weapon Systems Engineering, Defense Systems Division. Member AIAA.

Introduction

RECENT studies[1,2] have indicated military and civil needs for vertical lift of payloads exceeding the payload capacity of existing and anticipated heavy-lift helicopters. Military needs include lifting heavy battlefield equipment and off-loading container ships over undeveloped shores. Examples of civil applications include logging and transport and emplacement of heavy equipment for large construction projects. Use of multiple rotor vehicles appears to be a cost-effective method of lifting these heavy payloads since such vehicles can use existing helicopter propulsion and rotor systems. Hybrid aircraft employing rotor systems and a buoyant lifting hull appear to be particularly attractive, especially for extremely heavy lift, owing to the relatively lower cost of buoyant lift.

Consequently, a new generation of vertical takeoff and landing vehicle concepts, particularly rotorcraft with unprecedented lifting capability, is being developed[3] to airlift payloads externally on a sling. A particular concept that belongs to this class of aircraft and offers the possibility of greatly improved low-speed control and station-keeping characteristics far beyond that of historical lighter-than-air vehicles is the quad-rotor hybrid airship. Basically, this concept consists of a nonrigid, buoyant, nonrotating hull that is rigidly attached to a structural frame supporting the propulsion components. The advantage of such an arrangement is that the empty weight of the vehicle is supported by the force due to buoyancy while the propulsive forces are entirely available for lifting the payload and controlling the vehicle.

Since the quad-rotor airship is a novel vehicle concept, it is proposed to design and build a small-scale flight research vehicle called the buoyant quad-rotor aircraft (BQRA) for ground and flight test to prove the feasibility of the concept and investigate its flying qualities. In this article, the stability characteristics of such a flight research vehicle are discussed.

The extent of stability and control augmentation desirable for this aircraft depends on the inherent stability characteristics of the vehicle configuration. Consequently, its stability has been evaluated in typical flight conditions of hover and cruise. The effects of carrying a sling load on the vehicle dynamics have been predicted by considering a linear, state-variable model of the coupled system. Typical operational conditions that could lead to vehicle instability have been determined by using a flight dynamics simulation of the aircraft. The analytical model used and the determined

stability characteristics of the vehicle are described below, following a description of the aircraft itself.

Vehicle Description

Based on a preliminary design study,[4] a vehicle configuration was selected that would use existing hardware and thereby minimize the cost of the aircraft. The proposed configuration consists of four modified Hughes OH-6A helicopters mounted on the outriggers of an interconnecting structure that is attached to a conventional airship like the Goodyear blimp which has an envelope with an empennage as shown in Fig. 1. In this vehicle, the main rotor torques are countered by built-in tilt of the main rotor shafts of the helicopters, augmented by vehicle control moments when necessary.

As an option, it is proposed to hinge the helicopters in roll only to obtain additional thrust vectoring capability. Further, four auxiliary propellers, which are in fact tail rotors from the Bell helicopters Sea Cobra (AH-1T), are incorporated so that two of them augment the cruise mode of the vehicle while the other two augment the lateral control of the vehicle (see Fig. 1). These tail rotors were selected instead of conventional propellers so that 100% reverse thrusting capability could be provided to enhance vehicle control. In order to determine the effect of vehicle buoyancy on its flight characteristics, it is designed to be closer to neutral buoyancy while it is empty and is 10,000 lb heavy with maximum payload at sea level. Note that heaviness of the vehicle corresponds to gross weight in excess of static lift for that flight condition. The estimated physical properties of the aircraft are given in Table 1.

Mathematical Model

A linear system model which describes the coupled motion of the aircraft-sling load configuration, following a disturbance in its equilibrium flight path corresponding to hover or forward flight, is used to examine the associated stability characteristics. Such a model was obtained[5] by linearizing the corresponding nonlinear equations of motion of the vehicle and its sling load. The aircraft equations of motion are similar[6,7] to those of a buoyant vehicle. They are augmented to include the effect of a sling load. The following simple physical model of the configuration was used to obtain the corresponding mathematical representation.

Basically, the hull is assumed to be a buoyant, rigid body from which a payload, modeled here as a point mass, is suspended from an arbitrary point on the vehicle by means of a rigid, nonextensible link. The rotor modules in the configuration are assumed to be implicit devices that produce forces and moments on the vehicle for a specified flight path of the aircraft and appropriate control inputs.

Translation of the vehicle is described in terms of its velocity components u, v, and w along the x, y, and z axes, respectively, of a body axes system whose origin is located at the center of buoyancy of the aircraft; the rotational motion of the vehicle is described by the angular velocity components p, q, and r about the x, y, and z axes, respectively, of the same reference frame. The orientation of the vehicle is described by Euler angles ϕ, θ, and ψ, which locate the body axes reference frame with respect to a local horizon system.[8]

Motion of the payload relative to the vehicle is described in terms of its coordinates, x_p, and y_p, which are defined in the reference body axes system of the vehicle. Only two independent coordinates are required to describe the payload motion, since it is assumed that the payload remains at a constant distance, equal to the cable length, from the suspension point.

The corresponding perturbation equations are rearranged in a state-variable form:

$$\dot{\tilde{x}} = A\tilde{x}$$

where $\tilde{x}^T = [\Delta u\ \Delta w\ \Delta q \Delta\theta \Delta u_p \Delta x_p \Delta v\ \Delta p\ \Delta\phi\ \Delta r\ \Delta\psi\ \Delta v_p\ \Delta y_p]$ is the state vector consisting of perturbations in the state variables and A is the system matrix.

Typically, the stability characteristics of the system are determined by examining the eigenvalues of the system matrix. Stability characteristics of the vehicle alone, without a sling load, have been examined by appropriately partitioning the overall system matrix and using corresponding input data in the evaluation.

To examine the stability of the vehicle with an internal or external payload of 5000 lb while hovering or cruising, it is necessary to determine the corresponding aerodynamic derivatives of the vehicle. These have been synthesized by combining the aerodynamic derivatives of the quad-helicopter configuration with those of the airship component.

The contribution from the former has been determined by kinematically relating the individual helicopter derivatives[9] to those of the overall vehicle. In the present case, since the helicopter tail rotors are absent, their contribution to the aerodynamic derivatives of individual helicopters has been omitted. Consequently, as a first approximation, the yaw moment derivatives of individual helicopters have been neglected. The resulting contribution from the quad-helicopter configuration is shown in Table 2.

The contribution from the airship component has been estimated[10] before and is used directly. The acceleration derivatives (Table 3) corresponding to the airship component of the vehicle were estimated using classical approach.[11,12] The overall aerodynamic derivatives of the complete vehicle are given in Table 4. Based on these results, it can be seen that this vehicle has aerodynamic damping characteristics and cross-coupling effects similar to those of a conventional helicopter. The inherent static instabilities associated with a conventional airship in its pitching ($M_w > 0$) and yawing ($N_v < 0$) motions exist for the BQRA also. However, for the present vehicle the corresponding damping moments (M_q, N_r) are favorably augmented by the quad-helicopter contributions.

Table 1 Physical properties of the BQRA

Item	Estimate/ design value
Overall length	192 ft
Maximum width	100 ft
Maximum height	60 ft
Envelope volume (stretched)	205,270 ft^3
Helicopter rotor diameter	26 ft
Auxiliary propeller diameter	8 ft
Static lift (at sea level density altitude)	13,035 lb
Maximum gross weight (at sea level density altitude)	23,435 lb
Moments of inertia (includes 2258 lb of helium and an internal payload of 5075 lb)	
I_{xx}	363,961 slug-ft^2
I_{yy}	822,276 slug-ft^2
I_{zz}	1,030,234 slug-ft^2

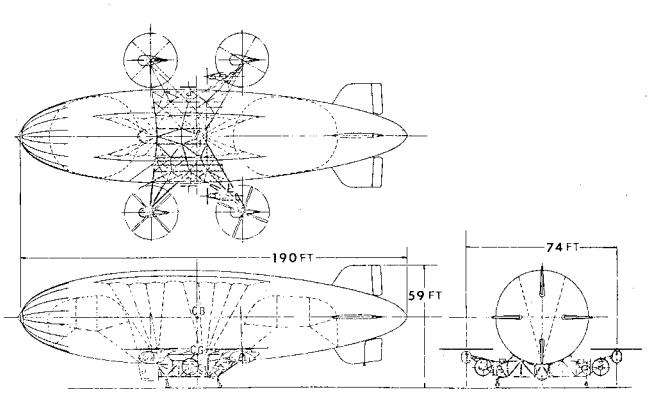

Fig. 1 Buoyant quad-rotor aircraft configuration.

Table 2 Quad-helicopter contribution to vehicle stability derivatives

	u	v	w	p	q	r
Hover at sea level:						
X	−8.15	0.12	3.58	−261.6	270.2	−19.27
Y	5.00	−13.79	−6.15	−184.93	−179.75	108.68
Z	−13.38	−13.95	−107.92	263.13	−229.47	467.54
L	−87.47	181.1	105.38	−134367.0	1664.8	14105.0
M	−97.6	−7.12	41.26	−3071.76	−55445.4	6982.5
N	...	...	...	−4388.6	3113.7	−16963.0
Forward flight at 20 knots at sea level:						
X	−5.29	0.76	6.84	−260.38	388.12	−31.35
Y	2.53	−15.54	−1.93	−228.28	−208.23	153.32
Z	−60.11	−11.73	−137.5	205.15	−1004.1	484.09
L	−43.83	213.92	24.97	−170212.0	2163.05	70601.2
M	−36.77	6.51	109.33	−3189.77	−68575.9	5731.65
N	...	...	...	−8388.86	−979.06	−14350.4
Forward flight at 40 knots at sea level:						
X	−8.56	0.25	3.96	−242.1	398.62	−17.53
Y	1.3	−21.52	−3.80	−234.08	−260.16	151.58
Z	−29.83	−7.41	−199.7	0.89	−687.54	459.26
L	−25.3	314.55	43.83	−246595.0	2897.35	33602.5
M	−103.4	−34.39	57.29	−2539.7	−101509.0	4110.95
N	...	...	...	−4854.7	1926.01	−21384.1

Table 3 Estimated acceleration derivatives of the aircraft

Derivative	Estimated value
$X_{\dot{u}}$	−37.1
$Y_{\dot{v}}$	−438.6
$Y_{\dot{r}}$	1489.8
$Z_{\dot{w}}$	−438.6
$Z_{\dot{q}}$	−1489.8
$M_{\dot{w}}$	−1489.8
$M_{\dot{q}}$	−687357
$N_{\dot{v}}$	1489.8
$N_{\dot{r}}$	−687357

Stability in Hover

For a case in which the vehicle was hovering in still air with an internal payload of 5074 lb, the corresponding system matrix was evaluated. It was found that the aircraft is inherently stable in this operating condition and has the following modal characteristics. In understanding these modes it is perhaps of interest to compare them with corresponding modal properties of a conventional airship[13,14] and a conventional helicopter.[15,16]

Mode 1 is a stable oscillation of the vehicle in the pitch plane with a time period of 16.1 s and time to half amplitude ($T_{½}$) of 37.1 s. The corresponding mode-shape (Fig. 2) indicates a phase relationship in which a change in forward velocity of 1 ft/s is associated with a change in pitch angle of 2.1 deg, the former leading the latter by 90 deg. The phase relationship observed here is similar to that of the pitch plane oscillation of the OH-6A helicopter in free flight.

Mode 2 represents heave subsidence with a $T_{½}$ of 7.8 s. It consists of vertical motion of the vehicle, which is damped by the helicopter rotors. In fact this mode is similar to the heave damping mode of a conventional helicopter.

Mode 3 represents surge subsidence with a $T_{½}$ of 70 s. It consists of convergence of the forward velocity of the vehicle resulting from surge damping of the individual helicopters. This mode is also similar to the surge subsidence mode of a helicopter except for the coupling with the pitch attitude observed in the latter case.

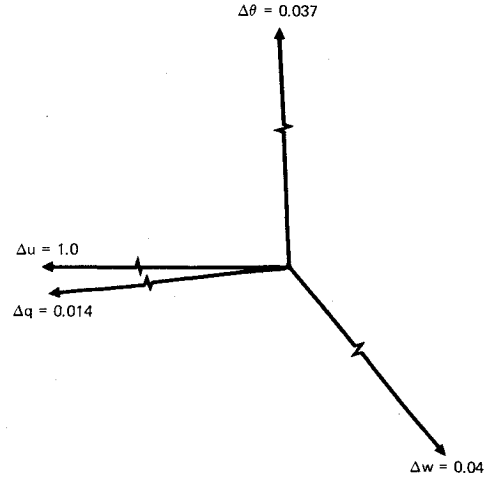

Fig. 2 Mode-shape of inherent longitudinal oscillation (Mode 1).

Mode 4 is a stable oscillation of the vehicle in the lateral vertical plane. It is well-damped and has a time period of 8.9 s with $T_{½}$ of 5.8 s. The corresponding mode-shape (Fig. 3) indicates that the resulting motion is predominantly rolling. A change in roll attitude of 10.3 deg is associated with a change in lateral velocity of 1 ft/s. This mode resembles the rolling oscillation observed in a conventional airship, more than the dutch-roll oscillatory mode of a helicopter.

Mode 5 is a heavily damped, weak oscillation of the vehicle in the horizontal plane. It has a time period of 560 s and a $T_{½}$ of 62.3 s. The corresponding mode-shape (Fig. 4) indicates coupled motion of the vehicle in which nearly equal changes occur in surge and sway velocities that are 180 deg out of phase. Small drift in heading was also observed in this case. This mode is perhaps unique to BQRA since it is not typically observed in conventional airships or helicopters.

Table 4 Estimated stability derivatives of the complete vehicle

	u	v	w	p	q	r
Hover at sea level:						
X	−8.15	0.12	3.58	−261.6	270.2	−19.27
Y	5.00	−13.79	−6.15	−184.93	−179.75	108.68
Z	−13.38	−13.95	−107.92	263.13	−229.47	467.54
L	−87.47	181.1	105.38	−134367.0	1664.8	14105.0
M	−97.6	−7.12	41.26	−3071.76	−55445.4	6982.5
N	...	...	...	−4388.6	3113.7	−16963.0
Forward flight at 20 knots at sea level:						
X	−27.33	7.91	13.99	−260.38	388.12	−31.36
Y	2.53	−157.79	−1.93	−228.28	−208.23	6944.02
Z	−60.11	−11.73	−279.76	205.16	−10255.6	484.09
L	−43.82	213.92	24.97	−170212.0	2163.05	70601.2
M	−36.77	6.51	5631.93	−3189.77	−839104.9	5731.65
N	...	−7662.7	...	−8388.86	979.06	−676809.0
Forward flight at 40 knots at sea level:						
X	−52.64	14.55	18.26	−242.1	389.62	−17.53
Y	1.3	−306.04	−3.80	−234.08	−260.16	13732.98
Z	−29.83	−7.41	−484.22	0.89	−19190.54	459.26
L	−25.3	314.55	43.83	−246595.0	2897.35	33602.5
M	−103.4	−34.39	11102.49	−2539.7	−1642567.0	4110.95
N	...	−15325.4	...	−4854.7	1926.0	−1346302.0

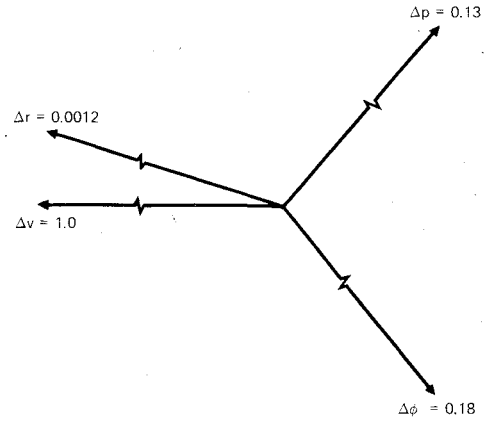

Fig. 3 Mode-shape of inherent lateral oscillation (Mode 4).

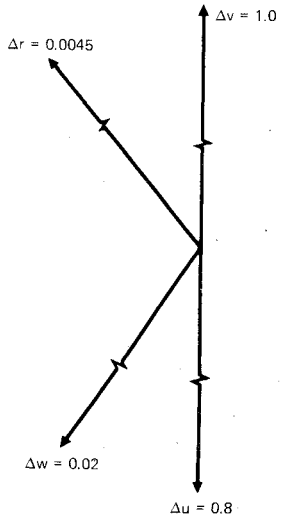

Fig. 4 Mode-shape of inherent, coupled longitudinal/lateral oscillation (Mode 5).

Stability in Forward Flight

In straight and level flight with increasing speed up to 40 knots, the pitch plane oscillation or Mode 1 (Fig. 5) tends to have a larger time period with greater damping. This behavior is similar to that of a conventional airship as shown in Fig. 6. For reference, the corresponding mode of a conventional helicopter is also shown in Fig. 6.

The increase in time period or decrease in natural frequency of oscillation for this vehicle at higher speeds can perhaps be explained as follows: As flight speed increases, the resulting aerodynamic pitch stiffness is destabilizing and hence tends to offset the inherent metacentric stability of the airship envelope. The net result is a reduction in the overall pitch stiffness of the vehicle, which leads to an increase in the period of oscillation. However, the pitch damping resulting from the empennage, as well as the quad-helicopter configuration, increases with speed. This results in a more dynamically stable vehicle at higher speeds.

The heave subsidence (Mode 2) tends to have greater damping at higher speeds, since the inherent heave damping of the individual helicopters increases with flight speed. This is characteristic of both conventional helicopters and airships.

The convergence of the longitudinal velocity component (Mode 3) observed in hover was found to become weakly divergent with time to double amplitude of 166 s in a flight at 20 knots. At higher speeds around 40 knots, however, this mode was again found to be convergent. The tendency towards instability at low speeds observed in this mode is not typical of airships or helicopters whose corresponding mode in fact tends to be more stable with increasing flight speed.

The oscillatory mode of the vehicle in the lateral vertical plane (Mode 4) remains stable in forward flight, with increasing damping at higher speeds up to 40 knots. This increase in damping results from the increased roll damping of the quad-helicopter configuration at higher speeds. The corresponding mode-shape is shown in Fig. 7 for a flight speed of 40 knots. The effect of varying flight speed on this mode has been found to be similar to that of a conventional airship as shown in Fig. 8. The corresponding mode of a helicopter in free flight is included in Fig. 8 for reference purposes.

The coupled longitudinal-lateral oscillation (Mode 5) observed in hover was found to decompose in forward flight

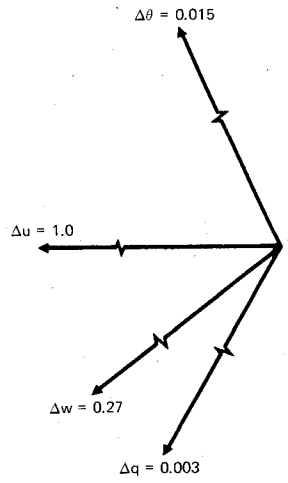

Fig. 5 Mode-shape of inherent longitudinal oscillation (Mode 1) in forward flight at 40 knots.

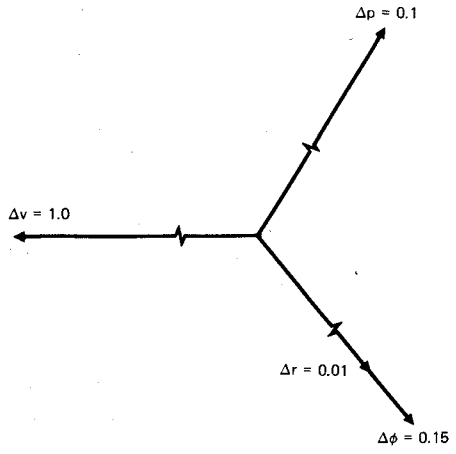

Fig. 7 Mode-shape of inherent lateral oscillation (Mode 4) in forward flight at 40 knots.

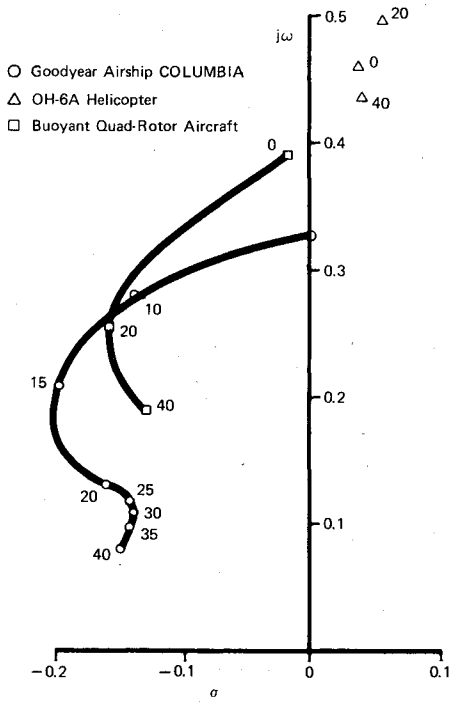

Fig. 6 Flight speed effect on pitch plane oscillation.

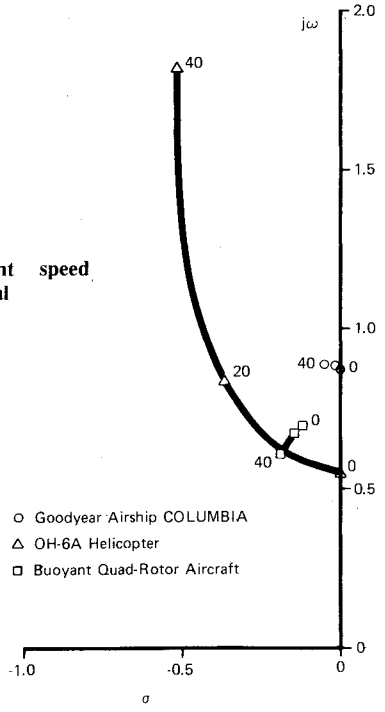

Fig. 8 Flight speed effect on lateral oscillation.

into aperiodic convergences of yawing and lateral-roll velocity of the aircraft. These subsidences are similar to yaw damping and roll damping modes of both helicopters and airships. The rolling subsidence tends to be more stable at higher flight speeds of the BQRA just as observed in the case of a helicopter or an airship. The yawing convergence mode tends to become more stable at higher speeds similar to that of an airship and unlike that of a helicopter.

Vehicle-Sling Load Stability

For a case in which the aircraft was hovering in still air with a sling load of 5074 lb ($K=0.2$), at the end of a 200-ft cable, the corresponding modes of the configuration have been determined. Here, the sling load was assumed to be suspended from a point on the vehicle that is vertically below the vehicle center of buoyancy ($z_s=26$ ft).

It was found that introduction of a sling load results in two additional oscillatory modes of vehicle-sling load motion in the longitudinal plane (Fig. 9) and in the lateral plane (Fig. 10). In addition, the inherent oscillatory modes of the vehicle were also found to become coupled with the corresponding sling load motions without causing any change in their modal properties. It was observed that in hover the sling load induced longitudinal oscillation (Mode 6) tends to be more unstable[17] for increasing suspension cable lengths up to 500 ft, while it remains stable in forward flight (Fig. 11). The lateral oscillation induced by the sling load (Mode 7) was found to be stable both during hover and forward flight with heavier damping occurring at higher forward speeds (Fig. 12).

Potential Instabilities

Typical operational conditions anticipated for this vehicle, such as those occurring during sling load pickup and dropoff as well as V/STOL modes of flight and cruise, were simulated to gain insight into potential stability problems. A six-degree-of-freedom flight dynamics simulation[4] previously developed for hybrid airships was used for this purpose.

Significant insight into maneuver stability of the aircraft was obtained by considering vehicle response to its control inputs in an open loop fashion. Initially, the vehicle by itself (gross weight of 18,018 lb) was trimmed in hover and subjected to individual unit step inputs to each of its controls with the open-loop results recorded on strip charts. A similar

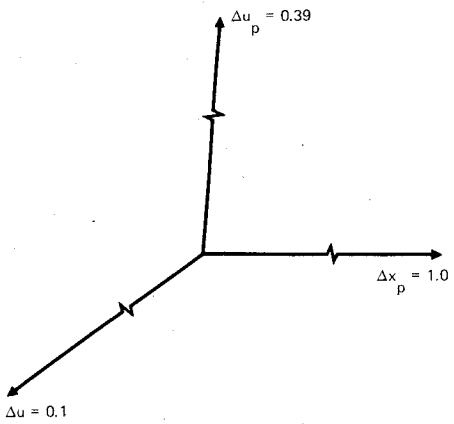

Fig. 9 Mode-shape of sling load induced longitudinal oscillation (Mode 6) in hover.

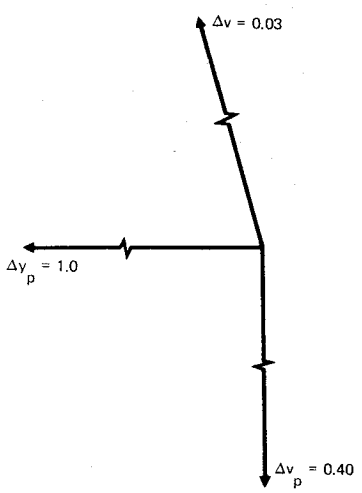

Fig. 10 Mode-shape of sling load induced lateral oscillation (Mode 7) in hover.

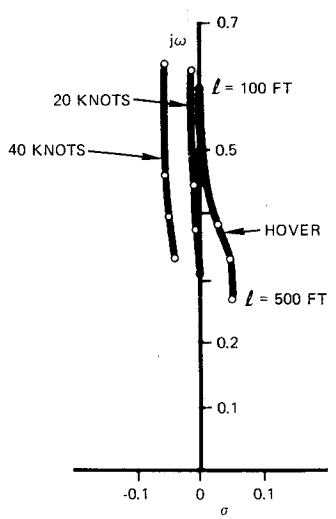

Fig. 11 Cable length effect on sling load induced longitudinal oscillation (Mode 6).

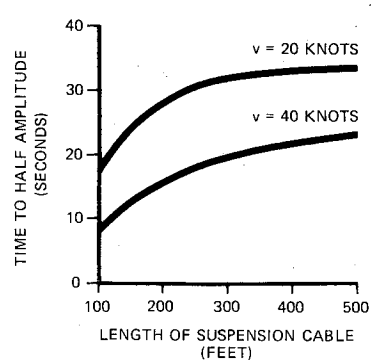

Fig. 12 Cable length effect on sling load induced lateral oscillation (Mode 7).

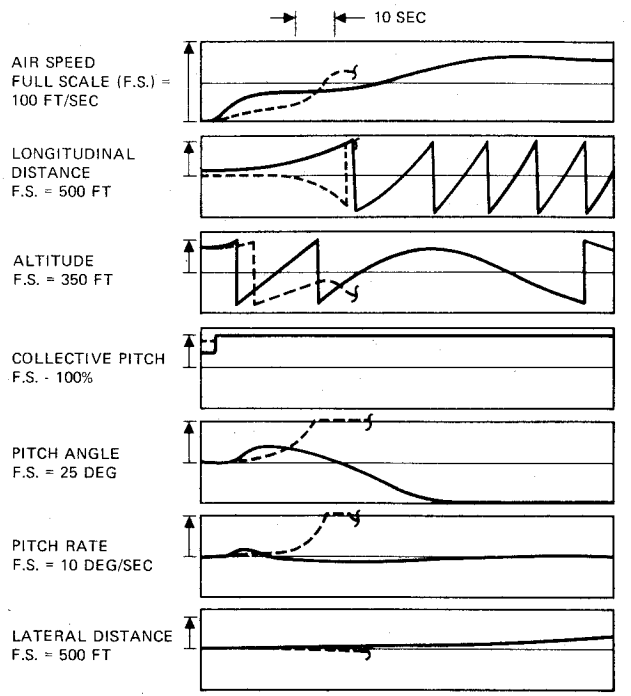

Fig. 13 Open loop response of the aircraft to a unit step input to its vertical control.

procedure was repeated for a case in which the vehicle was carrying an additional internal payload of 4274 lb.

Aircraft response to a unit step input to its vertical control, which is basically collective pitch input to all the four helicopter main rotors, is shown in Fig. 13. In this case both aerodynamic and dynamic cross-couplings in vertical and pitching motions are found which result in longitudinal motion as well. This can perhaps be explained as follows: Initially, as the aircraft climbs vertically it experiences an aerodynamic nose-up pitching moment which results in a pitch velocity. In conjunction with the prevailing vertical velocity this produces forward motion of the vehicle which decreases its angle of attack. Consequently, the vehicle experiences a nose-down pitching moment which results in a pitch-down attitude and a forward descent.

However, the vehicle with payload (shown by the dotted line in Fig. 13) responded by pitching up while drifting upward and backward, until it turned over. The backward motion in this case is perhaps due to the vehicle weight in excess of static lift, which tends to accelerate the climbing vehicle backwards if not countered. The net effect on the vehicle is a continuous nose-up tendency. A careful examination of the corresponding flight path reveals that vehicle motion in such a case is aerodynamically unstable. A detailed analysis should be conducted to verify this tendency. In any event, control and piloting techniques can be evolved that would overcome this problem. For instance, inherent vehicle trim in hover can be made to occur with a negative pitch attitude, which eliminates this flight regime.

Concluding Remarks

It should be observed that the basic modes of the vehicle described here already have been predicted[17,18] for similar configurations of this vehicle concept. However, the aerodynamic data used in all cases are preliminary[13] in nature. For instance, the aerodynamic interference between airship and helicopter components has not been accounted for. Consequently, a detailed stability analysis should be conducted after pertinent aerodynamic data have been generated for this vehicle. Albeit the vehicle is basically stable in hover and cruise flight modes, it is perhaps desirable to augment its stability, particularly during hover and low-speed flights.

It has been determined that the vehicle is sensitive to pitch disturbances while maneuvering near hover and climbing, and that this could eventually cause the aircraft to pitch over if not properly controlled.[19] This aspect of vehicle stability needs further evaluation before flight safety can be ensured.

Similarly, backward motion of the vehicle, if not properly controlled, has also been found to eventually lead to aircraft pitchover. However, piloted simulations involving these flight conditions have been conducted[20,21] successfully both with and without stability augmentation.

Acknowledgments

This research was conducted for NASA Ames Research Center under Contract NAS2-10777 monitored by P.D. Talbot. It is also based upon work conducted for the Goodyear Aerospace Independent Research and Development Program. The author is thankful to N.P. Tomlinson for his help in preparing and using the computer software, and to Dr. J.J. Hogan for his support and encouragement during this endeavor.

References

[1] "Alberta Modern Airship Study Final Report," prepared for Alberta Ministry of Transportation, Goodyear Aerospace Corporation, Akron, Ohio, GER-16559, June 1978.

[2] Mettam, P.J., Hansen, D., Byrne, R.W., and Ardema, M.D., "A Study of Civil Markets for Heavy Lift Airships," AIAA Paper 79-1579, July 1979.

[3] Williams, D.E., "The Development of a Heavy Lift Airship," American Helicopter Society Paper 80-9, May 1980.

[4] "Preliminary Design of a Hybrid Airship for Flight Research," NASA CR-166246, July 1981.

[5] Nagabhushan, B.L., "Linear System Definition of Heavy Lift Airship/Payload Configuration," Goodyear Aerospace Corporation, GER-16498, Akron, Ohio, Dec. 1977.

[6] Jones, S.P. and Krausman, J.A., "Nonlinear Dynamic Simulation of a Tethered Aerostat," AIAA Paper 81-1340, July 1981.

[7] Strumpf, A., "Equation of Motion of a Submerged Body with Varying Mass," Davidson Laboratory, Stevens Institute of Technology Report 771, May 1960.

[8] Miele, A., *Flight Mechanics, Vol. 1, Theory of Flight Paths*, Addison-Wesley, Inc., Palo Alto, Calif., 1962.

[9] Heffley, R.K., Jewell, W.F., Lehman, J.M., and Van Winkle, R.A., "A Compilation and Analysis of Helicopter Handling Qualities Data," NASA CR-3144, Aug. 1979.

[10] Bezbatchenko, J.W., Davis, R.J., and Sowa, W.W., "GZ20(G/L) Airship Stability and Control," Goodyear Aerospace Corporation, GER-13844, Akron, Ohio, May 1968.

[11] Lamb, H., *Hydrodynamics*, Dover, New York, 1945.

[12] Imlay, F.H., "The Complete Expressions for Added Mass of a Rigid Body Moving in an Ideal Fluid," David Taylor Model Basic Report 1528, July 1961.

[13] Curtiss, H.C., Hazen, D.C., and Putnam, W.F., "LTA Aerodynamic Data Revisited," *Journal of Aircraft*, Vol. 13, Nov. 1976, pp. 835-844.

[14] Delaurier, J. and Schenk, D., "Airship Dynamic Stability," AIAA Paper 79-1591, July 1979.

[15] Bramwell, A.R.S., *Helicopter Dynamics*, John Wiley, New York, 1976.

[16] Johnson, W., *Helicopter Theory*, Princeton University Press, Princeton, N.J., 1980.

[17] Nagabhushan, B.L. and Tomlinson, N.P., "Flight Dynamics Simulation of a Heavy Lift Airship," *Journal of Aircraft*, Vol. 18, Feb. 1981, pp. 96-102.

[18] Tischler, M.B., Jex, H.R., and Ringland, R.F., "Simulation of Heavy Lift Airship Dynamics Over Large Ranges of Incidence and Speed," AIAA Paper 81-1335, July 1981.

[19] Nagabhushan, B.L., Lichty, D.W., and Tomlinson, N.P., "Control Characteristics of a Buoyant Quad-Rotor Research Aircraft," AIAA Paper 81-1838, Aug. 1981.

[20] Talbot, P.D., Miura, H., and Tucker, G.E., "Piloted Simulation of a Buoyant Quad-Rotor Aircraft," AIAA Paper 81-1345, July 1981.

[21] Nagabhushan, B.L. and Tomlinson, N.P., "Piloted Simulation of a Heavy Lift Airship with a Sling Load," Dec. 1981, Goodyear Aerospace Corporation, GER-17010, Akron, Ohio, Dec. 1981.